Iraqi Journal of Science, 2025, Vol. 66, No. 10, pp: 4644 – 4660
DOI: 10.24996/ijs.2025.66.10.44

ISSN: 0067-2904

Calculation of the Best Date for Transfer Orbit with Perturbation from (GTO) to Lagrange Point (L2)

Omar A. Fadhil , Abdul-Rahman H. Saleh
Department of Astronomy and Space - College of Science - University of Baghdad, Iraq

Received: 20/5/2024 Accepted: 20/10/2024 Published: 30/10/2025

Abstract

Lagrange points are points where the gravity of two large celestial bodies does not affect a third body, usually smaller, making its motion follow the motion of the two large bodies. There are five points relative to the Earth, the Sun, and any third body, such as a satellite or a spacecraft. Three essential points are usually symbolized as L1, L2, and L3. This research aims to calculate the best date in 2025 for the satellite to transition from the GTO orbit to the L2 Lagrange point, another transition station to transfer the satellite from (L2) to the Mars orbit. A program was designed in MATLAB to calculate the best date 2025 for the satellite to transition from the Geosynchronous Transfer Orbit (GTO) to the L2 Lagrange point during a transition orbit between the Earth orbit (GTO) to the Sun orbit L2. This requires reaching the escape velocity from the Earth orbit and then the extinction velocity when the spacecraft arrives near L2 in the presence of three types of perturbations: solar gravitational perturbation, the effect of the third body, and the perturbation of the Earth's non-sphericity J2. The results showed that the best date for the transition is Monday, October 2, 2025, because the required velocity for the transition is suitable. The perturbation effect on the orbital elements is small compared to other dates. The transition time is 35.34 days. This means that the departure day will be Monday, Monday, October 2, 2025, and the arrival will be Monday, March 17, 2025. Although there are other dates for the satellite transition with the shortest transition time, the perturbation on the orbital elements of the transition orbit is higher. The perturbation effect on the orbital elements of the transition orbit depends on the satellite's mass. The greater the satellite's mass, the less the effect of perturbation on it, and vice versa.

Keywords: Lagrange points, Geosynchronous Transfer Orbit (GTO), Third body effect, solar attraction.

حساب أفضل تاريخ للمدار الانتقالي مع الاضطراب من (GTO) إلى نقطة لاغرانج (L2)

عمر عامر فاضل ، عبدالرحمن حسين صالح
قسم الفلك والفضاء، كلية العلوم، جامعة بغداد ، بغداد، العراق

الخلاصة

نقاط لاغرانج هي نقاط لا تؤثر فيها جاذبية جسمين سماويين كبيرين على جسم ثالث، عادة ما يكون أصغر، مما يجعل حركته تتبع حركة الجسمين الكبيرين. هناك خمس نقاط بالنسبة للأرض والشمس وأي جسم ثالث، مثل القمر الصناعي أو المركبة الفضائية. عادة ما يرمز إلى ثلاث نقاط أساسية بـ L1 وL2 وL3. يهدف هذا البحث إلى حساب أفضل تاريخ في عام 2025 لانتقال القمر الاصطناعي من مدار GTO إلى نقطة

*Email: om19ar95@gmail.com

لاغرانج L2، وهي محطة انتقال أخرى لنقل القمر الاصطناعي من (L2) إلى مدار المريخ. تم تصميم برنامج في MATLAB لحساب أفضل تاريخ 2025 لانتقال القمر الاصطناعي من مدار النقل الجغرافي المتزامن (GTO) إلى نقطة لاغرانج L2 أثناء مدار انتقالي بين مدار الأرض (GTO) إلى مدار الشمس L2. وهذا يتطلب الوصول إلى سرعة الهروب من مدار الأرض ومن ثم سرعة الانقراض عند وصول المركبة الفضائية بالقرب من L2 في وجود ثلاثة أنواع من الاضطرابات: اضطراب الجاذبية الشمسية، وتأثير الجسم الثالث، واضطراب عدم كروية الأرض J2. وأظهرت النتائج أن أفضل موعد للانتقال هو يوم الاثنين 2 أكتوبر 2025، لأن السرعة المطلوبة للانتقال مناسبة. وتأثير الاضطراب على العناصر المدارية صغير مقارنة بالتواريخ الأخرى. وزمن الانتقال هو 35.34 يومًا. وهذا يعني أن يوم المغادرة سيكون يوم الاثنين 2 أكتوبر 2025، وسيكون يوم الوصول يوم الاثنين 17 مارس 2025. وعلى الرغم من وجود تواريخ أخرى لانتقال القمر الاصطناعي بأقصر زمن انتقال، إلا أن الاضطراب على العناصر المدارية لمدار الانتقال أعلى. ويعتمد تأثير الاضطراب على العناصر المدارية لمدار الانتقال على كتلة القمر الاصطناعي. كلما زادت كتلة القمر الاصطناعي، كلما كان تأثير الاضطراب عليه أقل، والعكس صحيح.

1. Introduction:

Lagrange points are points in space where transmitting objects, like satellites, tend to remain stationary. At Lagrange points, the centripetal force of a tiny body traveling alongside two massive mass bodies equals the gravitational force. Figure 1 shows the Lagrange points, which satellites use to lower the fuel needed to maintain their position in space.

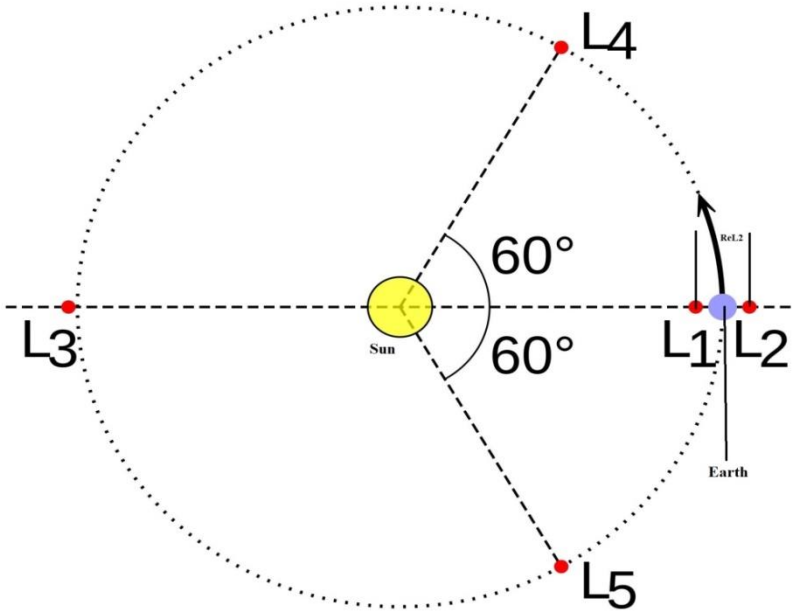

Figure 1: The Lagrange points of Earth's orbits relative to the Sun [1].

Since the Earth is a solar system, all planets and other components are primarily under the influence of the sun's gravity. However, there is another effective force acting on the Earth, like the moon and other planets, proportional to their mass and distance from the Earth, to study these cases mathematical equations for gravitational effect upon the mentioned body under study. The need for space exploration and satellite and space telescope technology led to the study of the optimum place for these space tools around Earth orbital. Several physics and classical mechanics methods were introduced to examine these places, such as two-body (in 1609, the two-body problem was analyzed by Johannes Kepler and solved by Isaac Newton in 1687). The three-body problem, which is the problem of taking the initial velocities and

positions (or momenta) of three-point masses and solving for their motion following Newton's laws of motion and Newton's law of universal gravitation, is the more straightforward and realistic case in which the three body problem was studied [1]. One particular instance of the n-body problem is the three-body problem. In the past, the Earth, Sun, and Moon three-body problem was the first particular three-body problem to be thoroughly studied [2]. To find the differential equations that would account for the motion of the bodies, Newton initially investigated the concept in 1687. Although numerous other researchers have investigated the issue, Poincare's seminal work in 1890 marked a significant advancement [3]. There are typically 18 first-order differential equations in a three-body problem. It can be whittled down to 6 using maths and conservation equations. Because there aren't enough conservation quantities to support further simplification, the problem hasn't been addressed yet. Looking at more limited examples to understand what would happen in constrained situations is best. Two massive masses orbit their shared center of mass in a circle in the restricted three-body problem. There is the entry of a third body into the system, which is considerably smaller than the other two. The challenge is determining how this object will move as it is affected by the gravitational pull of the larger bodies. The circular restricted three-body issue applies to many circumstances in the solar system. The eccentricity of the Earth's orbit around the Sun is 0.0167, and the Moon's orbit around Earth is 0.0516; the old dates make their orbits essentially circular [4].

Previous research and studies on this topic focused on geostationary orbit (GEO), medium Earth orbit (MEO), and low Earth orbit (LEO) satellites, such as GPS and GLONAS, which were studied by Sue in 2000 [5]. The effects of atmospheric drag and zonal Harmonics on the orbits of satellites in low Earth orbit is a study by Al-Burmani and S. Barron (2009), which concluded that there is no apparent effect of the J2 spherical harmonics of the gravitational potential during the early stage of injection. The dominant effect was the drag force in the atmosphere at the perigee, which decreased the satellite's altitude until its return after 1560 days in a dense atmosphere [6]. In the year (2017) Allam, Awad, and Amin calculated the Bi-Elliptic Hohmann transfer and one tangent burn transfer calculations using Monte Carlo simulation. In 2020, Mahdi, Saleh, and Jarad studied determination and published an article whose main objective was to evaluate the orbital transition methods between two elliptical earth orbits.

The U.S. National Aeronautics and Space Administration (NASA) led Webb's design and development and partnered with two central agencies: the European Space Agency (ESA) and the Canadian Space Agency (CSA). The NASA Goddard Space Flight Center in Maryland managed telescope development, while the Space Telescope Science Institute in Baltimore on the Homewood Campus of Johns Hopkins University operates Webb. The primary contractor for the project was Northrop Grumman. He Webb was launched on 25 December 2021 on an Ariane 5 rocket from Kourou, French Guiana. In January 2022, it arrived at its destination, a solar orbit near the Sun-Earth L2 Lagrange point, about 1.5 million kilometers (930,000 mi) from Earth. The telescope's first image was released on 11 July 2022. The telescope is named after James E. Webb, who was the administrator of NASA from 1961 to 1968 during the Mercury, Gemini, and Apollo programs [7].

The importance of this research is that having a project to transfer a satellite from Earth to Mars, and this research is one of the steps to transition to L2 because it is low voltage and through which the transfer to Mars is done, and expect that the energy difference in this method will be less than direct transfer.

In this research, the Hohmann method was used for transition. The Hohmann transfer method is an elliptical orbit that contacts both inner and outer orbits, and the transfer orbit from

the perigee or apogee of the initial orbit to the final orbit is direct in half a period. The Hohmann transfer methods have different efficiency for two-impulse maneuvers and depend on the height of the initial orbit.

Table 1: Types of satellites (space telescopes) that reached Lagrange points

Satellites Lagrange points EARTH/SUN	Date	L1	L2	L3	L4	L5
SOHO (Solar and Hemispheric Observatory)	1995	•●				
ACE (Advanced Composition Explorer) space-borne energetic particles from the Sun-Earth	1997	●●				
DSCOVR (Deep Space Climate Observatory) is an American space weather station that monitors changes in the solar wind, providing space weather alerts and forecasts for geomagnetic storms.	1998	●●				
WMAP(The Wilkinson Microwave Anisotropy Probe) to make the fundamental measurements of cosmology, the study of the properties of our universe as a whole	2001		●●			
GENESIS(probe that collected a sample of solar wind particles and returned them to Earth for analysis)	2001	●●				
PLANCK(study the Cosmic Microwave Background)	2009		●●			
HERSCHEL(the only space observatory that covered the spectral range from far–infrared to sub-millimeter Wavelengths)	2009		●●			
GAIA(Space Observatory (ESA) the spacecraft is designed for astrometry: measuring the positions, distances, and motions of stars with unprecedented precision and the positions of exoplanets by measuring attributes about the stars they orbit, such as their apparent magnitude and color)	2013		●●			
JWST(James Webb Space Telescope)	2022		●●			

The gravitational three-body problem is a special case of the circular restricted gravitational three-body Circular Restricted Gravitational Three-Body Problem (CRGTBP).

The n-body problem: The CRGTBP consists of three bodies; these two bodies (which are named the primaries or the primary and the secondary) move in a circular orbit about their center of mass's center influenced by gravitation between them with the infinitesimal mass body, which the third body move under their gravitational effect of the two masses where its mass could be negligent influence compared these two masses. Moreover, the common plane movement of the body is defined by both the primary and secondary [8][9][10].

The two larger bodies' masses are denoted as m_1 and m_2, and they are assumed to be traveling in a circle with a radius of r_{12} around each other under the influence of only their mutual gravitation. Consider a non-inertial, co-moving frame of reference (x, y,z) originating at the two-body system's center of mass (G); the z-axis is perpendicular to the orbital plane where the y-axis is located. m_1 and m_2 appear to be at rest in this frame of reference, as shown in Figure (2), where the constant inirtial angular velocity Ω is provided by [11].

$$= \sqrt{\mu/(r_{12})^3} \quad (1)$$

Since M is the total mass of the system, $M = m_1 + m_2$, $\mu_e = GM_e$, r_{12} is distance between m_1 and m_2

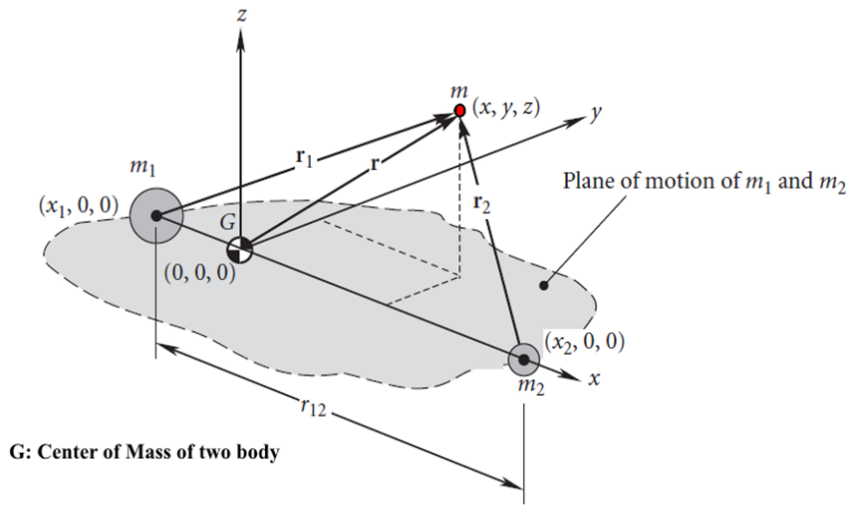

Figure 2: m_1 *and* m_2 are the two primary bodies that revolve around each other in a circular orbit, in addition to a secondary mass, m [11].

From the definition of the center of mass, the dimensionless mass ratios are given by

$$\pi 1 = m_1/M \quad , \quad \pi 2 = m_2/M \tag{2}$$

$\pi 1$ *and* $\pi 2$ represents the center of mass

This is known as the circular restricted three-body problem Circular Restricted Gravitational Three-Body Problem (CRGTBP) because the mass m is assumed to be so small that it does not affect the motion of the primary bodies. It introduces a third body of mass, m, which is vanishingly small compared to the primary mass. m_1 and m_2, like the mass of a spacecraft compared to that of a planet or moon in the solar system.

The secondary mass m location vector concerning m1 is provided by [11].

$$r_1 = (x - x_1)\hat{i} + y\hat{j} + z\hat{k} = (x + \pi 2\, r_{12})\hat{i} + y\hat{j} + z\hat{k} \tag{3}$$

About $m2$ the location vector of the secondary mass m is [11].

$$r_2 = (x - \pi 1\ r_{12})\hat{i} + y\hat{j} + z\hat{k} \tag{4}$$

The position vector of the secondary body relative to the center of mass is [11].

$$r = x\hat{i} + y\hat{j} + z\hat{k} \tag{5}$$

Let us observe that Newton's second law for the secondary body is

$$m\ddot{r} = F1 + F2 \tag{6}$$

$F_1 and\ F2$ are the gravitational forces exerted on $m_1 and\ m_2$, respectively.

$$F1 = -(Gm_1 * m)/(r_1)^3 * r_1$$
$$F2 = -(Gm_2 * m)/(r_2)^3 * r_2$$
$$If \quad \mu_1 = Gm_1 \quad , \quad \mu_2 = Gm_2$$

By substituting in equation (6), the acceleration relation is obtained.

$$\ddot{r} = -\mu_1/(r_1)^3 * r_1 - \mu_2/(r_2)^3 * r_2 \tag{7}$$

By substitute the inertial angular velocity and the position vectors in acceleration relation and by arranging the variables components and equating the coefficients of î,ĵ and k̂ on each side of this equation yields the three scalar equations of motion for the circular restricted three-body problem [11].

$$\ddot{x} - 2\Omega\dot{y} - \Omega^2 x = -\mu_1/(r_1)^3\,(x + \pi 2 * r_{12}) - \mu_2/(r_2)^3\,(x + \pi 1\, r_{12}) \tag{8-a}$$
$$\ddot{y} + 2\Omega\dot{x} - \Omega^2 y = \mu_1/(r_1)^3\, y - \mu_2/(r_2)^3\, y \tag{8-b}$$
$$\ddot{z} = -\mu_1/(r_1)^3\, z - \mu_2/(r_2)^3\, z \tag{8-c}$$

2- Methodology:

L2 will be included in our primary calculations since it is perfect for astronomy since a spacecraft can easily connect with Earth, maintain the Sun, Earth, and Moon behind the spacecraft for solar power, and give our telescopes a clear view of outer space.

Earth's orbit and the L2 point have an ellipse orbit around the Sun. Then, the distance and velocity are derived from the equation of motion, which is not exact because of the effect of other bodies (such as planets) on Earth.

The distance between the Sun and Earth at a given location in its orbit (during the year)R_{ES}, orbital equation was used [11].

$$R_{ES} = \frac{a_e(1-e_e^2)}{(1+e\cos\theta)} \quad (9)$$

Where a_e , e_e and θ represent the semi-major axis, eccentricity, and true anomaly of the Earth's orbit around the Sun.

On the other hand, the orbital velocity of the Lagrange points (L2) around the Sun was calculated using the orbital velocity equation [12].

$$V_L = \sqrt{\mu(\frac{2}{R_{EL2}} - \frac{1}{a_{L2}})} \quad (10)$$

Where $\mu_\odot$ represent $GM_\odot$ and R_{EL2} is the instantaneous distance from the Sun, which is calculated by adding R_{ES} and Lagrange points distance from Earth at time.

Another method was used to calculate the orbital velocity of the (L) using Newton's law of gravity.

$$\frac{M_E G}{R_{EL}^2} + \frac{M_\odot G}{R_{SL}^2} = \frac{V_{Or}^2}{R_{SL}} \quad (11)$$

Where V_{Or} , R_{EL} and R_{SL} represent the orbital velocity of the Lagrange point on its orbit around the Sun, the distances between the Earth and Lagrange point (L2), and the Sun and Lagrange point L2.

The following is the perturbed Equation of Motion (EOM) on the perturbed elliptical orbit [13]:

$\ddot{r} = \frac{d^2r}{dt^2}$ is the satellite acceleration at the time (t) in unit km/s^2.

$$\ddot{r} = -\frac{\mu}{r^3}\vec{r} + \ddot{r}_p \quad (12)$$

Where $\mu_e = G * M_e$=398603.4416 when the distance in km and the time in sec where G is the gravitational constant and Me is the Earth mass, $\vec{r}$ is the position vector for the satellite, and r is the distance between the earth's center and satellite at time (t) [11].

Where $\ddot{r}_p$ is the perturbation acceleration, which can be written as the following

$$\ddot{r}_p = \ddot{r}_E + \ddot{r}_s + \ddot{r}_M + \ddot{r}_{sp} + \ddot{r}_A \quad (13)$$

Where $\ddot{r}_E$ is the non-spherically and inhomogeneous mass distribution within Earth (central body), $\ddot{r}_s$ and $\ddot{r}_M$ is the Sun and the Moon acceleration attraction on the satellite, $\ddot{r}_{sp}$ acceleration due to Solar radiation pressure and $\ddot{r}_A$ acceleration due to atmospheric drag.

Two types of perturbations were used in this study (solar attraction, third body effect, and non-spherical Earth orbit J2) [14].

The solution of the equation (12) is give the satellite distance [15]:

$$r = \frac{h^2}{\mu}\frac{1}{1+ecos(f)} \quad (14)$$

h: angular momentum per unit mass f: True anomaly angle (0,360°).

From equation (3), the perigee and apogee distance r_p , r_a are derived at f= 0 and 180 degrees.

$$r_p = a(1-e) \quad (15A)$$

$$r_a = a(1+e) \quad (15B)$$

Where a is the semi-major axis of the elliptical orbit.

The eccentricity of the transfer orbit can be calculated by [15]:

$$e = \frac{r_a - r_p}{r_a + r_p} \quad (16)$$

Where r_a: is the distance between L2 and the Earth upon arrival time.
r_p: is the distance of the satellite from the Earth center at the start of the transition.
This equation was used to calculate the angular momentum [15].

$$\boldsymbol{h = \sqrt{2\mu}\sqrt{\frac{r_a - r_p}{r_a + r_p}}} \quad (17)$$

This equation calculates the velocity for an elliptical orbit [15].

$$v^2 = \mu\left(\frac{2}{r} - \frac{1}{a}\right) \quad (18)$$

The semi-major axis (a) can be calculated from equation (15A or 15B) [15].

The following equation may be used to determine the velocity needed to transfer the satellite from its initial orbit to its final orbit through the transition orbit. The change in velocity required to transition is represented by the symbol Δv [16].
Then, transition time is required. Equation (10) can be used to get the transition time where μ=398602.4415 at a, r in km, and the period in second, T_{trans}=1/2T.

$$T_{tran} = \frac{1}{2}\left(\frac{2\pi}{\sqrt{\mu}} a^{\frac{3}{2}}\right) \quad (19)$$

The mass of a satellite is not constant through transition orbit because of mass burn. This can be written as the following [15]:

$$\frac{\Delta m}{m} = 1 - e^{-\frac{\Delta v}{Isp\ go}} \quad (20)$$

Where:
Δ m is the consumed mass for propellant, g_o is the gravity standard of acceleration, and Isp is the impulsive specific of the propellants. The vectors perturbation accelerations on satellite is given as the following [17] [18]:

$$a_{J2} = \frac{-3\mu R_e^2 J_2}{2r^7}\begin{bmatrix} x(x^2 + y^2 - 4z^2) & . \\ y(x^2 + y^2 - 4z^2) & . \\ z(3x^2 + 3y^2 - 2z^2). \end{bmatrix} \quad (21)$$

Where (R_e) is the Earth radius (6372 km) and $(x, y, and\ z)$ are the components of the satellite position, r is the distance of the satellite. The J2 value for Earth is J2=1082.6283*10^{-6}.

4. Result and Discussion:

The MATLAB program designed a program to calculate the orbital elements of the primary and transitional orbit and the effect of disturbance on the orbital elements of the transitional orbit. The perturbed equation was solved using the 4th-order Runge–Kutta method. The most commonly used Runge-Kutta method to find the solution of a differential equation is the RK4 method, i.e., the fourth-order Runge-Kutta method. The Runge-Kutta method provides the approximate y value for a given point x. Only the first-order ODEs can be solved using the Runge Kutta RK4 method. (It is one of the integration methods to calculate velocity from acceleration or distance from velocity. It uses six values of the variable that are predicted by exchanging the function in the previous period [18][19][20].

Algorithm:

1. Calculated the (JD).
2. Calculate the Geocentric coordinates of the sun through the year.
3. Calculate the heliocentric coordinates of the Earth and L2 through one year.
4. Calculate the orbital element of the initial satellite orbit around the Earth.
5. Calculate the energy required Δv total,$T_{transition}$, Δm/m, for the transfer orbit from the orbit around the Earth to the orbit of L2 around the Sun.
6. Calculate orbital elements of transfer orbit with perturbations.
7. Calculate the best transfer orbit by changing the date of the start of the transfer.

These results, gated by equations (1,2,6,8,9,10,12,14,15A,15B,16,17,18,19,20,21), were written in Table (2). The change in the orbital elements of the transition orbit in the presence of perturbations shows these results for half a cycle, where it becomes clear to us that the orbital element most affected by perturbation is the semi-major axis, Figures (3, 4, 5, 6, 7, 8, 9, and 10). Each drawing represents a specific date and month for 2025 and the extent of the influence of the perturbations. The results showed that the best date for the transition is Monday, February 10, 2025, because the velocity required for the transition is appropriate, its small value about (Δv total = 4.17897268314359 km/s), which is the sum of the delta-v in the velocity required to transition from the GTO orbit and delta- V2, which is it represents the velocity that the satellite needs to brake and reduce its velocity when arriving near the Lagrange L2. The effect of the perturbation on the orbital elements is also tiny compared to the other dates. The time for transition is 35.3426225316822 days. This means the departure day will be Monday, February 10, 2025, and arrive on Monday, March 17, 2025. Although there are other dates to transition satellites in the shortest time of transition, the perturbation on the orbital elements of the transition orbit is high; for example, 10/3/2025 and 10/9/2025 need the time transition of about 32 days, but the perturbation is high the second result can be used if it is not possible to transition on the first date for technical reasons, for example.

Figure (11) shows the greatest effect of the perturbation on the inclination of the transfer orbit on 10/4/2025 and also on 10/10/2025 and the low value in inclination on 10/6/2025. As for its effect on the semi-major axis, it peaks on 10/6/2025. The reason for this is the influence of the third body, for example, the Moon and that effect will change due to a location change in the moon with the date, Figure (12). Figure (13) shows the omega angle effect by perturbation reached a higher value on 10/10/2025 and 10/4/2025; the true Anomaly's highest value is due to the perturbation effect on 9/10/2025, Figure (14). As for the Right Ascension of ascending node, it reaches its highest value on 12/10/2025 and its lowest value on 11/10/2025 in Figure (15). Eccentricity is the last element affected by the perturbation, with the highest value on April 10, 2025, Figure (16).

Table 2: The variation orbital elements of the transition orbit with different dates of starting the transfer.

date	Δi (deg)	Δa(km)	Δta (deg)	Δ Ω (deg)	Δ R.A (deg)	Δ e	T_{tran} (day)	Δv-total (km/sec)	Δm/m
10/1/2025	-0.096570046116	36643.26	0.2839	-0.5874572485546	31.57666506	-0.038556425	43.7210222	4.19608603	0.35134
10/2/2025	0.143669024351	-18424.71	3.057875642	0.39997943486	30.15419824	-0.05252574	35.3426225	4.17897268	0.35134
10/3/2025	0.361172048473	-37229.23	4.333510329	1.080090596497	30.02761118	-0.035736457	32.5138103	4.55247793	0.35134
10/4/2025	0.415492399989	-14079.23	2.540232367	1.159734576696	30.16205554	-0.027425428	34.6334693	4.64835892	0.35134
10/5/2025	0.196666356264	40388.27	3.153738258	0.2310957582995	29.73513856	-0.06061645609	42.6539720	3.89148699	0.35134
10/6/2025	-0.086343779043	72080.42	2.696899648	-0.9032896653568	31.20022590	-0.05233671454	50.3813008	3.85770463	0.35134
10/7/2025	-0.105089977225	40122.42	1.070179645	-0.6679581826523	31.62293744	-0.03885270303	44.5791399	4.17228050	0.35134
10/8/2025	0.098231714265	-11003.30	0.135837128	0.2425717326471	30.40591684	-0.04968914239	36.3701839	4.19498911	0.35134
10/9/2025	0.343408823610	-36409.34	5.167706593	1.050382618218	29.92434273	-0.03945252307	32.5356074	4.48209822	0.35134
10/10/2025	0.430963514856	-18903.51	1.931118037	1.220923428410	29.81861180	-0.03434047668	34.0288434	4.52966363	0.35134
10/11/2025	0.209636581771	41315.07	1.751306157	0.2027945633050	29.73337039	-0.06095015052	39.1622832	3.87682079	0.35134
10/12/2025	-0.100516043388	78646.20	0.409895866	-1.023019020900	31.92379582	-0.03560086204	52.0747522	4.07827249	0.35134

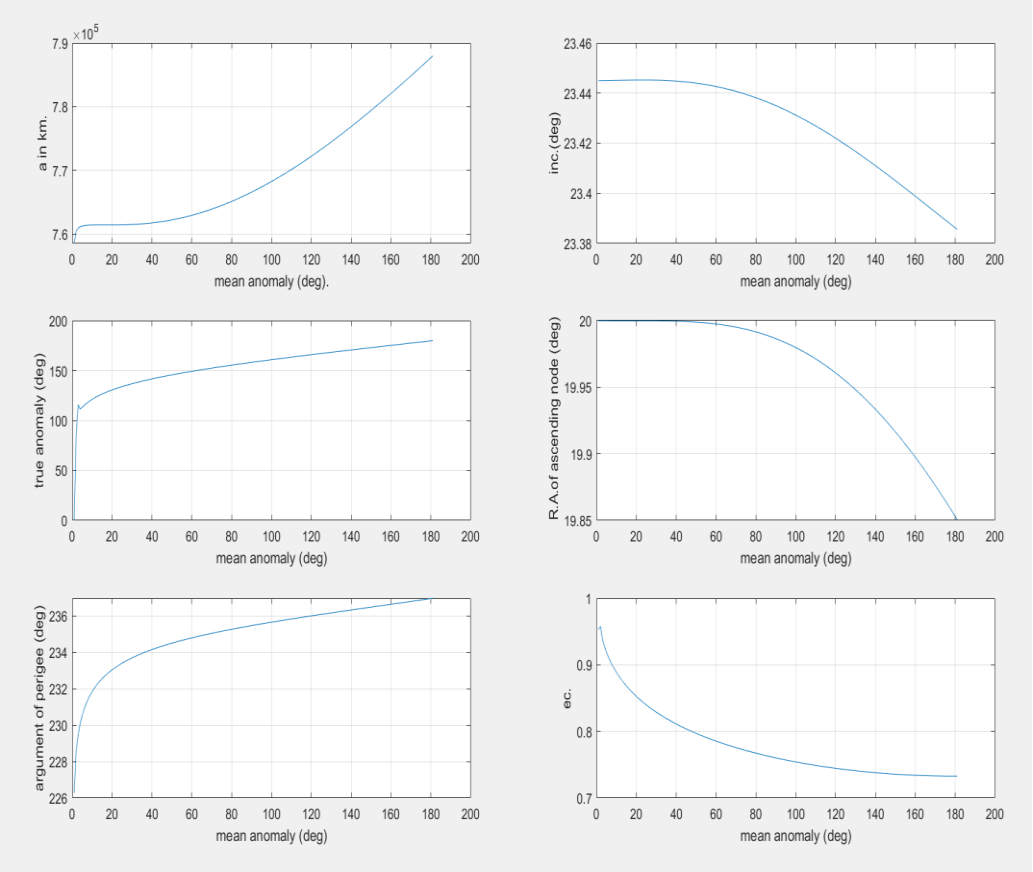

Figure 3: The variation orbital elements of the transition orbit on 10/1/2025.

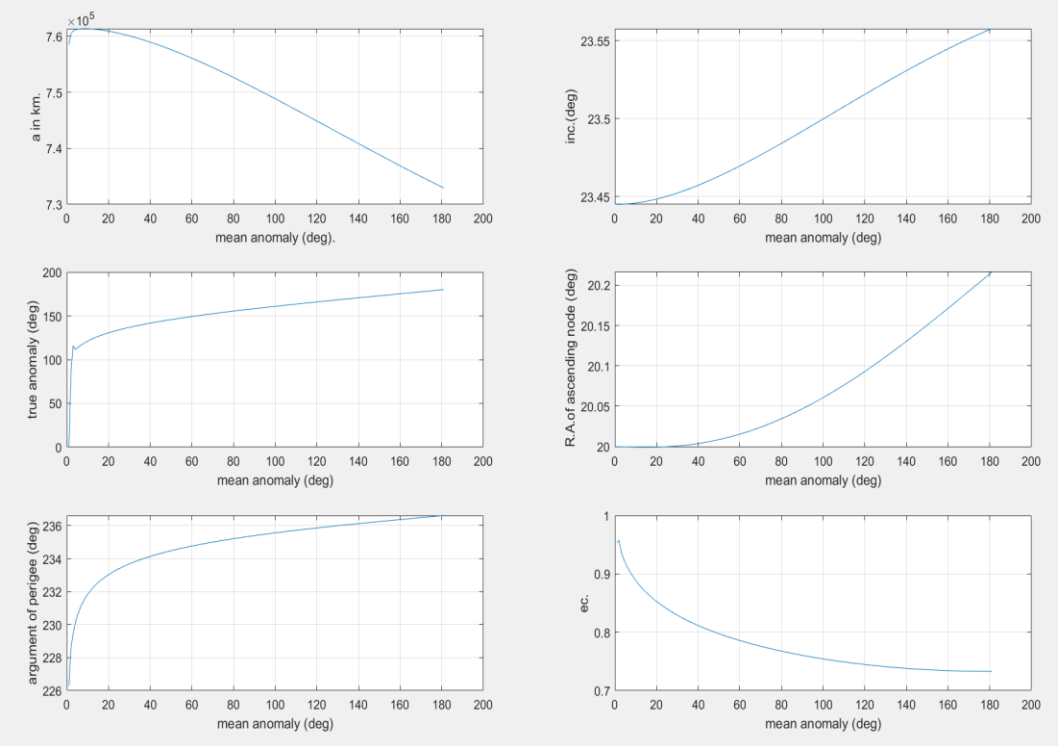

Figure 4: The variation orbital elements of the transition orbit in 10/2/2025

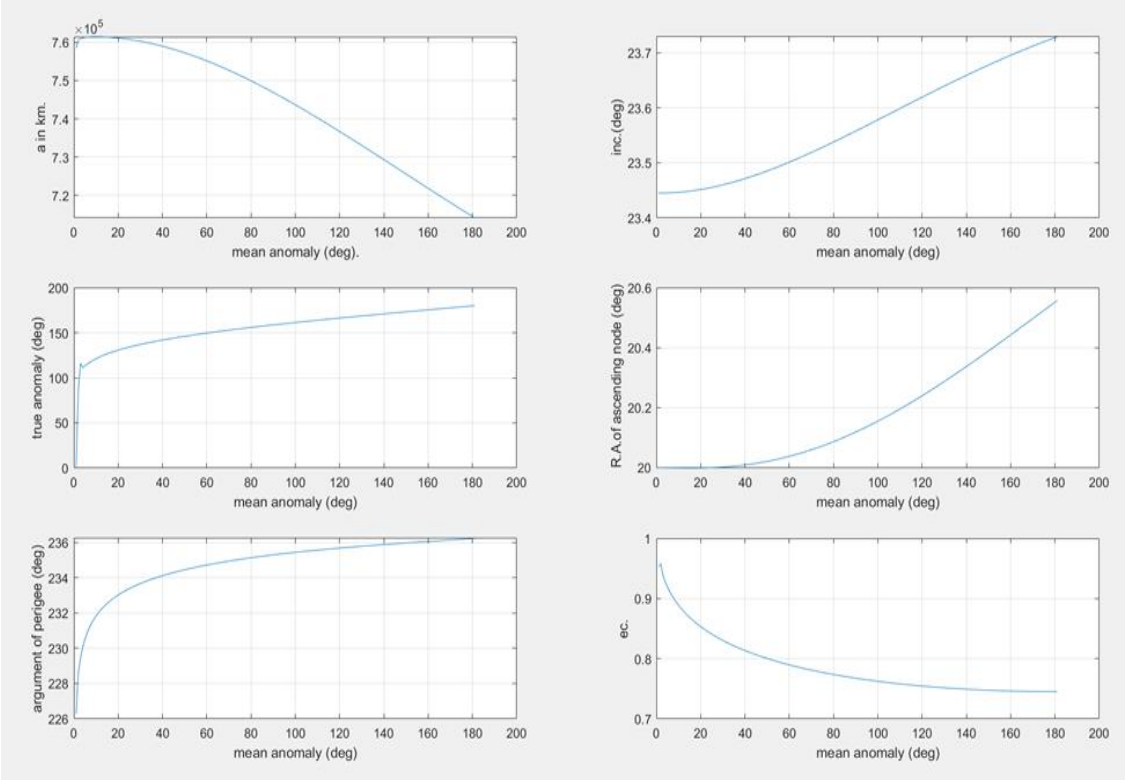

Figure 5: The variation orbital elements of the transition orbit in 10/3/2025

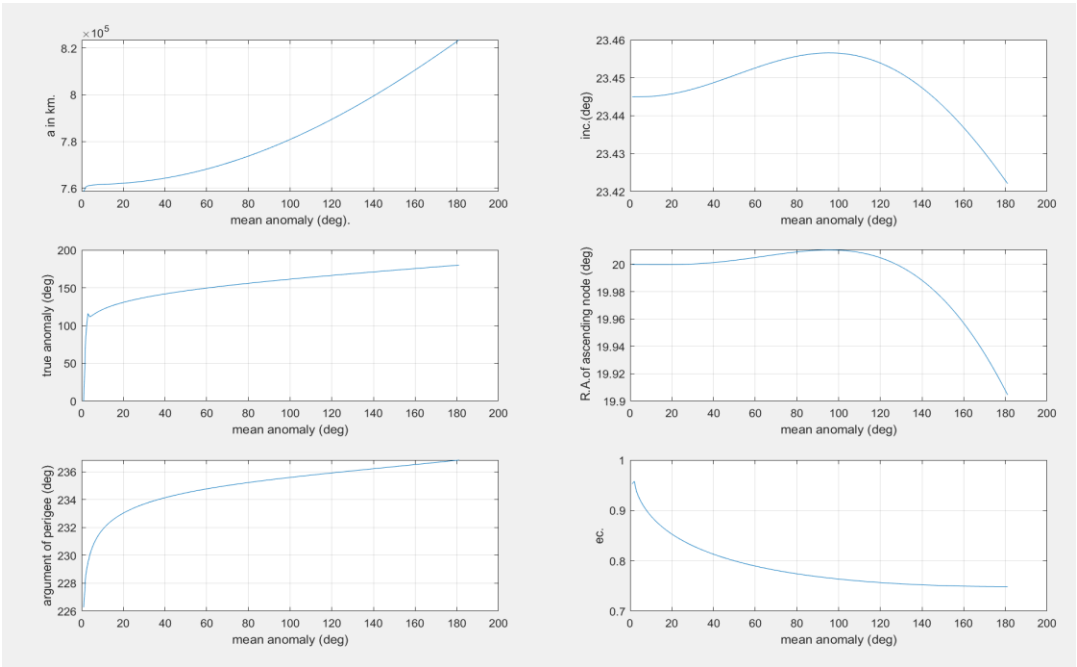

Figure 6: The variation orbital elements of the transition orbit on 10/6/2025

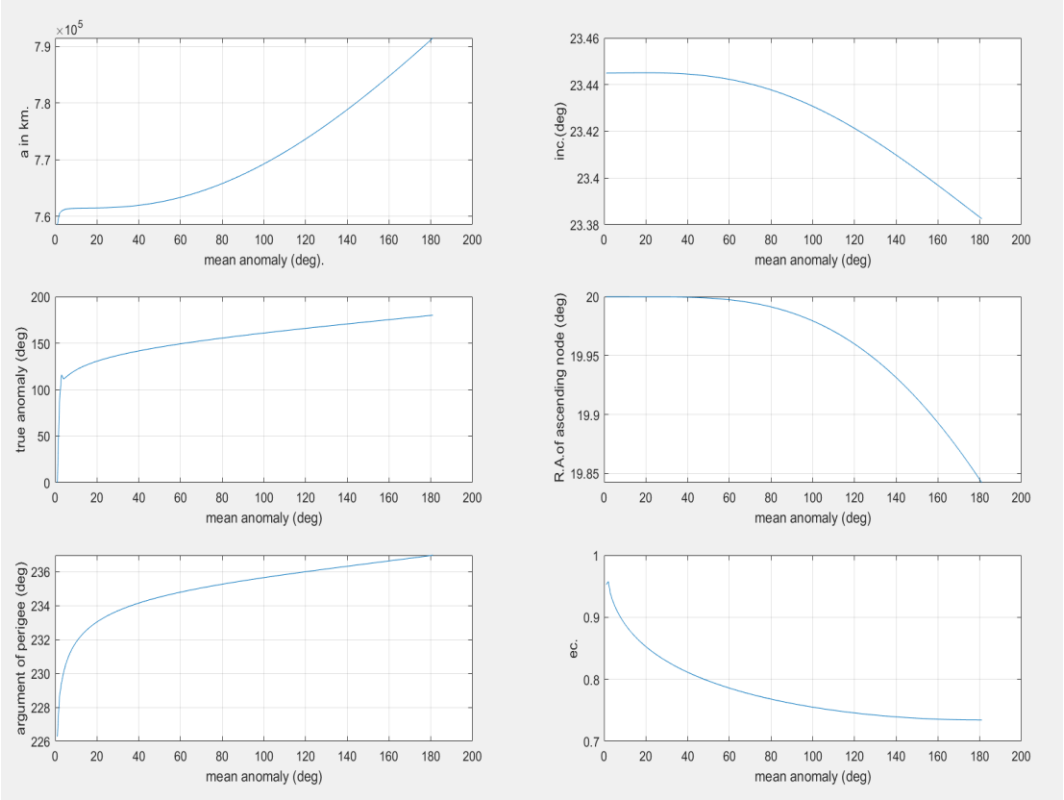

Figure 7: The variation orbital elements of the transition orbit on 10/7/2025

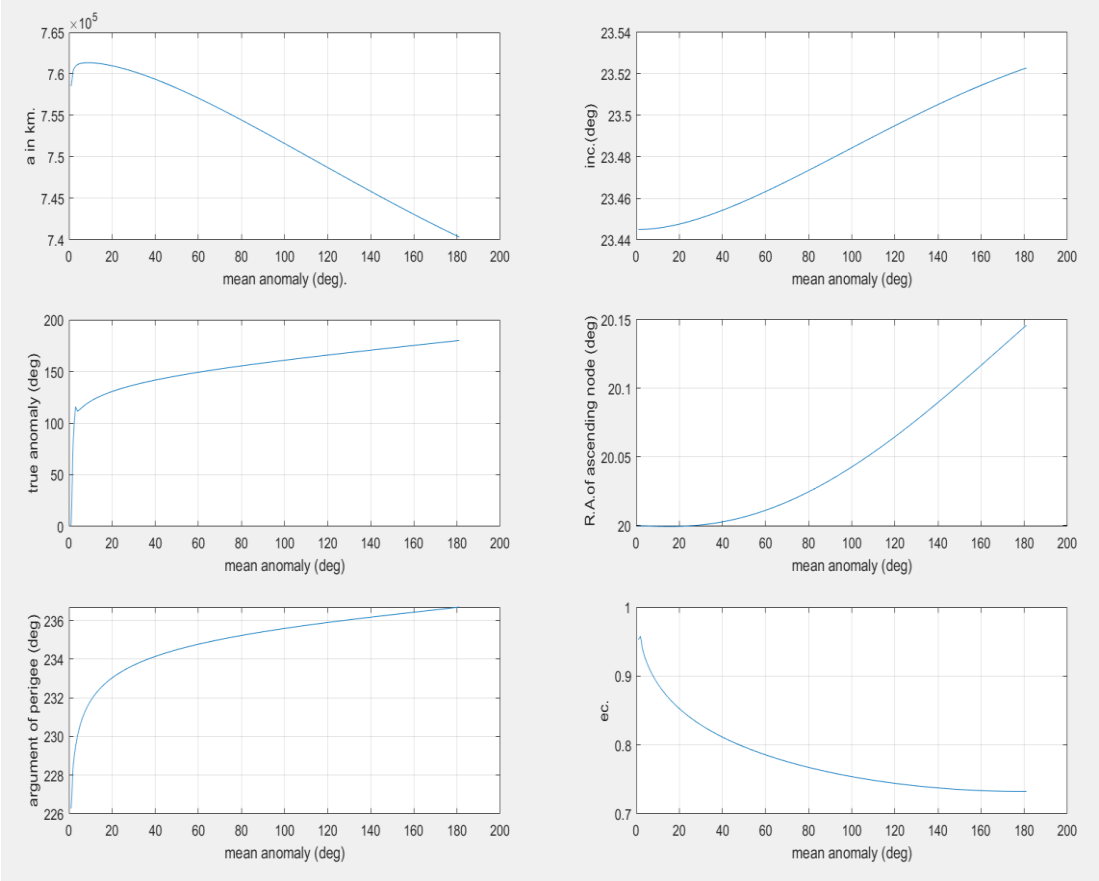

Figure 8: The variation orbital elements of the transition orbit on 10/8/2025

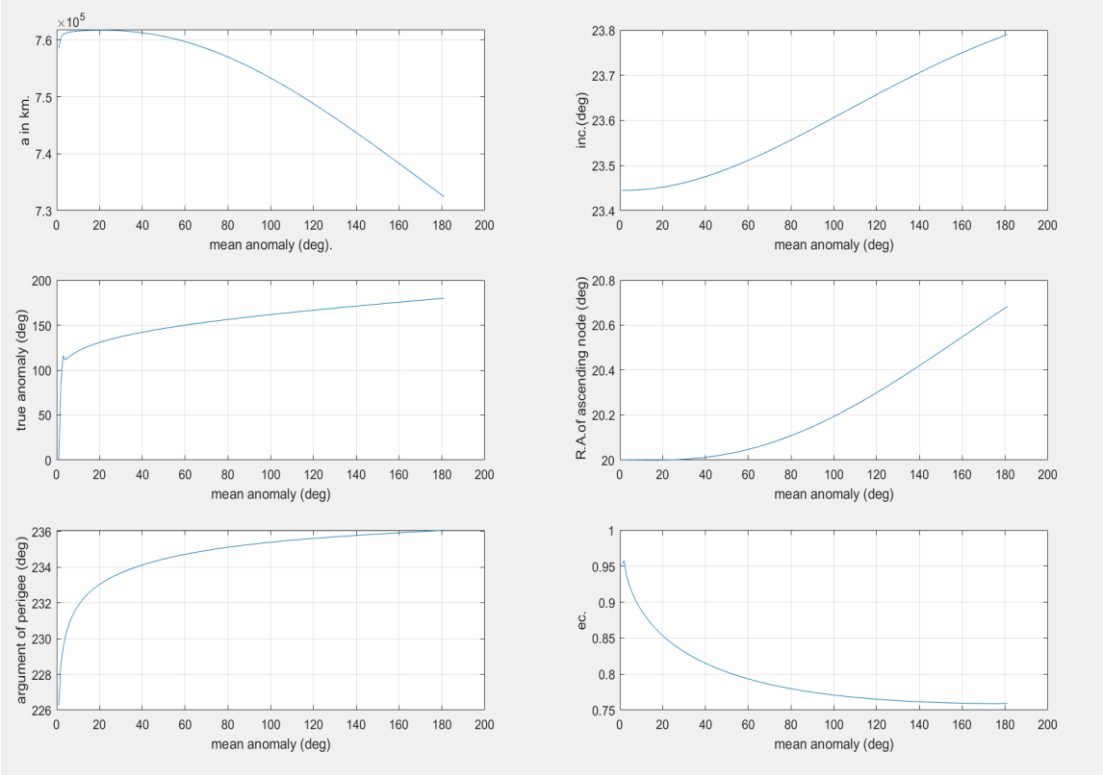

Figure 9: The variation orbital elements of the transition orbit on 10/10/2025

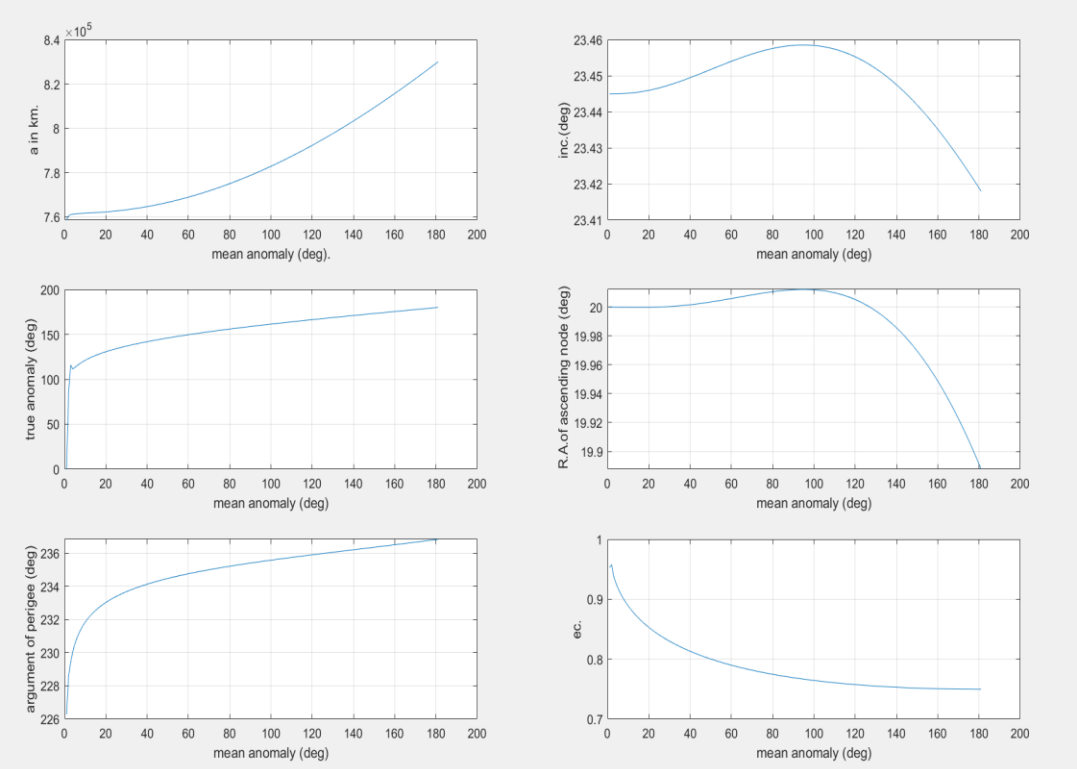

Figure 10: The variation orbital elements of the transition orbit on 10/12/2025

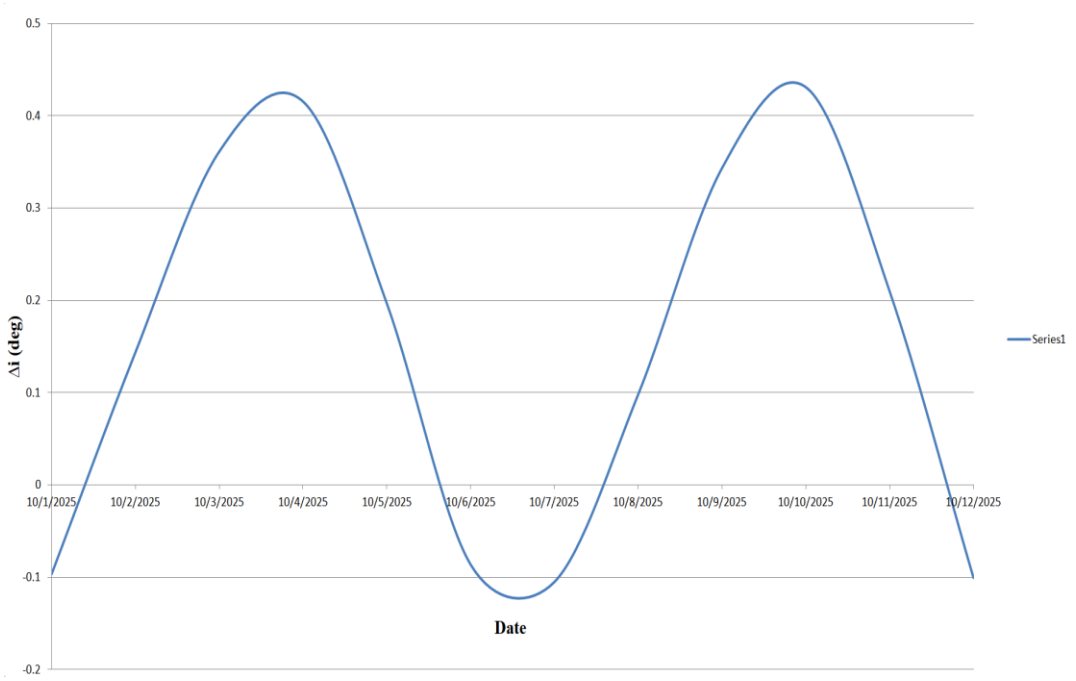

Figure 11: The variation inclination of the transition orbit with date

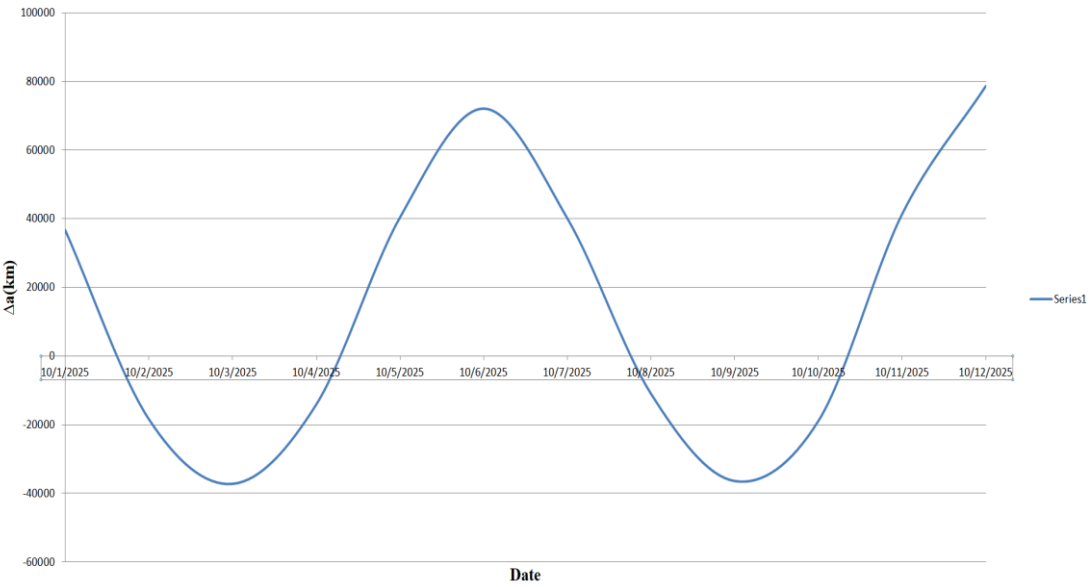

Figure 12: The variation semi-major axis of the transition orbit with the date

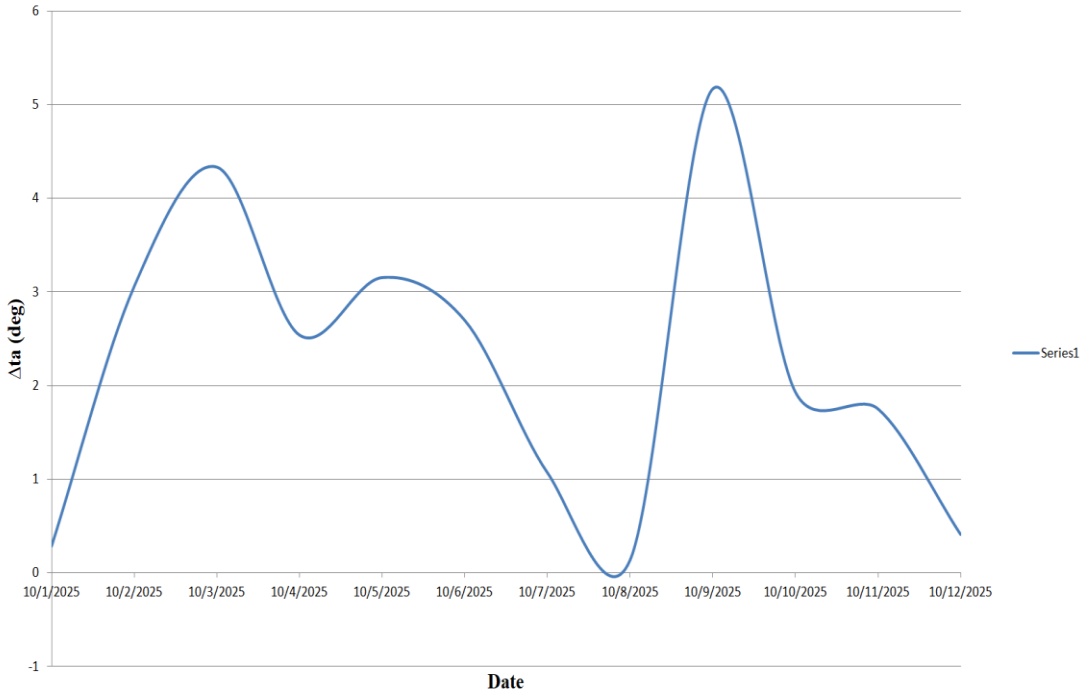

Figure 13: The variation true anomaly of the transition orbit with date

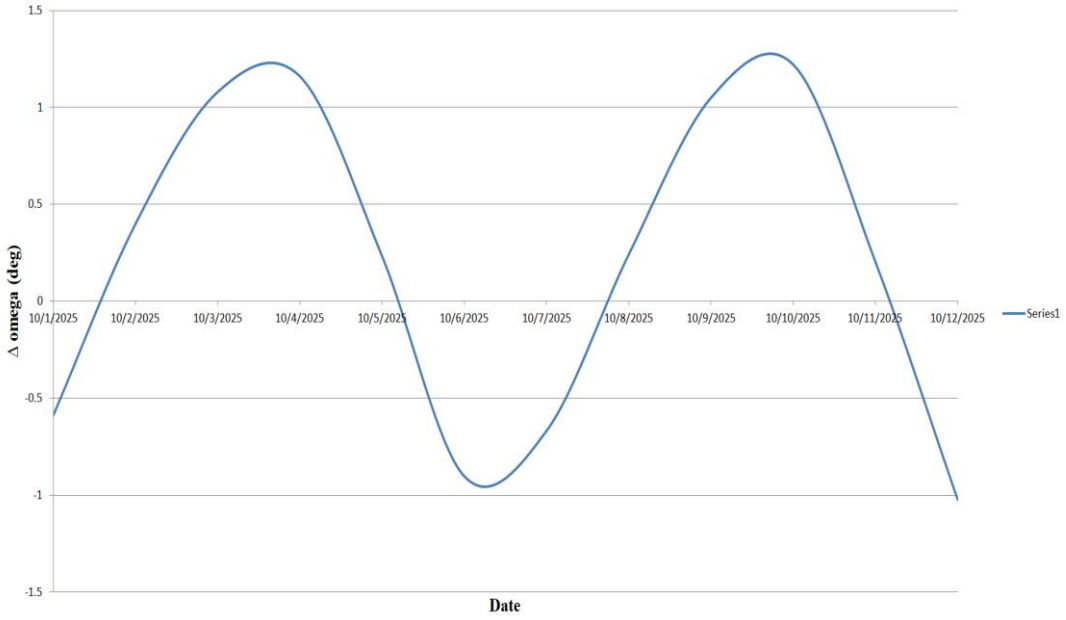

Figure 14: The variation omega of the transition orbit with date

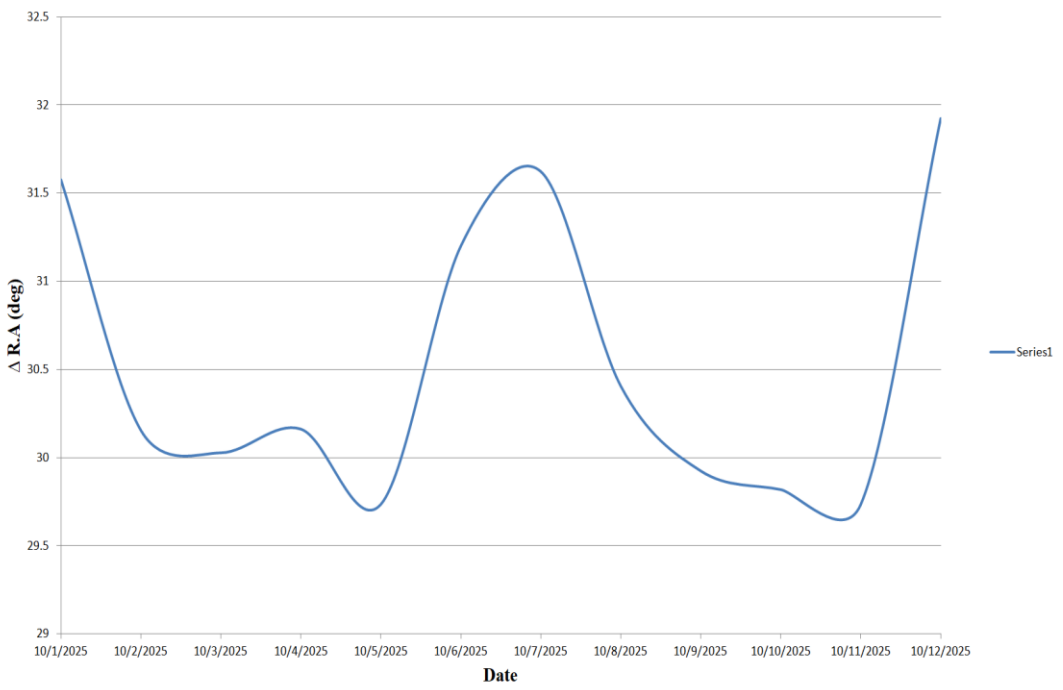

Figure 15: The variation R.A of the transition orbit with date

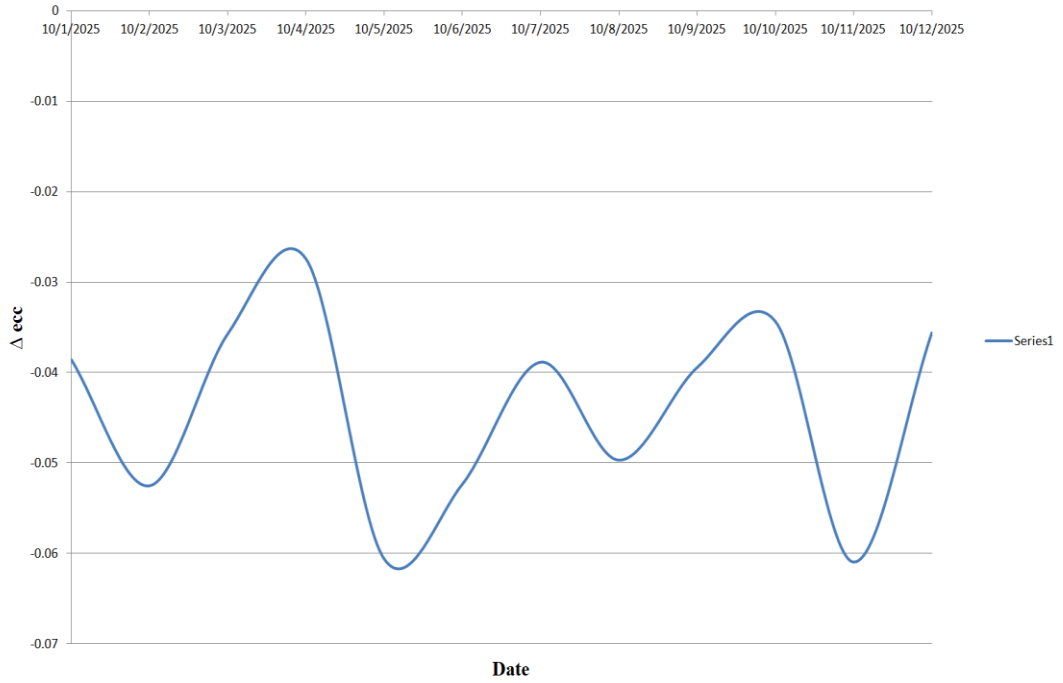

Figure 16: The variation eccentricity of the transition orbit with date

5-Conclusions:

In this research, several things were concluded:

The type of perturbation most affecting the orbital elements is the third-body effect, and the effect of perturbation increases with the mass of the satellite. It concludes that the best day to transition from GTO to Lagrange point L2 was chosen: February 10, 2025. The reason is that the impact of the perturbation is low compared to other dates, and the velocity required for the transition ΔV1 and the braking velocity ΔV2 are appropriate; the perturbations' effect on the transition orbit's orbital elements is small. Its effect is clear on the semi-major axis but cannot be neglected. The reason is the cumulative value. If the transition does not take place during

one cycle, its effect may be very clear; the advantage of studying the L2 is home to some of the most extraordinary space missions where the latest satellite to reach L2 is the James Webb Space Telescope (launched on 25 December 2021) and for any space station for starting point mission is to study nearby explants and explore the farthest reaches of the Universe to observe the very first galaxies, It is important to refer that calculation were done are approximately because its canceled the gravitational effect of planets and moon for simplicity.

References:

[1] T. Gowers, J. Barrow-Green, I. Leader. (2008, Sep 28). *The Three-Body Problem princeton-companion-to-mathematics* [online]. Available: https://press.princeton.edu/books/hardcover/9780691118802/the-princeton-companion-to-mathematics

[2] S. Wolfram, "A New Kind of Science," *Chaos Theory Wolfram Media, Inc*, p. 972, 2016.

[3] J. Barrow-Green, "Poincare and the Three Body Problem," *Am. Math. Soc.*, pp. 7, 45, 1997.

[4] R. Frnka, "The Circular Restricted Three-Body Problem," 2010, [Online]. Available: http://jan.ucc.nau.edu/~ns46/student/2010/Frnka_2010.pdf

[5] T. Hiriart, J.-F. Castet, J. M. Lafleur, and J. H. Saleh, "Comparative reliability of GEO, LEO, and MEO satellites," in *Proceedings of the International Astronautical Congress, IAC-09 D*, 2009.

[6] M. J. Al-Bermani, Aref S. Baron., "The Effects of Atmospheric Drag and Zonal Harmonic on LEO Satellite Orbits," *Babylon Univ. J.*, vol. 17, no. 2, Jan 2009.

[7] L. Fisher, Alise; Pinol, Natasha; Betz, "President Biden Reveals First Image from NASA's Webb Telescope," 2022.

[8] A. . Roy, "Orbital Motion," *CRC Press. Boca Raton, Florida*, 2004.

[9] J. Worthington, "A Study of the Planar Circular Restricted Three Body Problem and the Vanishing Twist," *Tese Doutorado, Univ. Sydney*, 2012.

[10] A. A. Alghamdi, M.H. and Alshaery, "A Series Solution Approach to the Circular Restricted Gravitational Three-Body Dynamical Problem," *J. Appl. Math. Phys.*, 2020.

[11] Howard D. Curtis. (2020). *Orbital Mechanics for Engineering Students* [online]. Available: https://www.sciencedirect.com/book/9780081021330/orbital-mechanics-for-engineering-students#book-info

[12] A.E. Roy and D. Clarke, *Astronomy: Principles and Practice*, 4th edition. 2003.

[13] G. Seeber. (2003, June 19). *Satellite Geodesy* [online]. Available: https://www.degruyter.com/document/doi/10.1515/9783110200089/html

[14] "Evaluation of Orbital Maneuvers for Transition from Low Earth Orbit to Geostationary Earth Orbit," *IRAQI J. Sci.*, vol. 59, no. 1A, Jan. 2018, doi: 10.24996/ijs.2018.59.1A.21.

[15] D. D. Abood."Calculation of the Appropriate Satellite or Elements around Mars," *Ph.D. thesis, Dep. Astron. Space, Coll. Sci. Univ. Baghdad,* 2023.

[16] M. Linick. (2016). *A General Method for Orbital Transfer Using Tangent Burns* [online]. Available: https://oer.pressbooks.pub/lynnanegeorge/chapter/chapter-7-manuvering/

[17] D. D. Abood and A. H. Saleh, "Calculation of the Best Stability Orbit of the Satellite around the Earth before Transferring to Orbit around Mars," *Iraqi J. Sci.*, pp. 4876–4891, Sep. 2023, doi: 10.24996/ijs.2023.64.9.45.

[18] D. A. Vallado, "Perturbed Motion," *Anal. Graph. Inc*, Dec. 2007, doi:10.1016/S1874-9305(07)80003-3

[19] R. H. Ibrahim, "Improvement of the Accuracy of the Perturbed Orbital Elements for LEO Satellite by Improving 4th Order Runge–Kutta's Method," *Indian J. Sci. Technol.*, vol. 13, no. 4, pp. 417–429, Jan. 2020, doi: 10.17485/ijst/2020/v13i04/148503.

[20] M. Capderou. (2014). *Handbook of Satellite orbit* [online]. Available: https://link.springer.com/book/10.1007/978-3-319-03416-4.